UWB Sensor Radar Networks for Indoor Passive Navigation

Stefania Bartoletti
CNIT, ENDIF, University of Ferrara
stefania.bartoletti@unife.it

Andrea Giorgetti
DEI, WiLAB, University of Bologna
andrea.giorgetti@unibo.it

Andrea Conti
ENDIF, WiLAB, University of Ferrara
a.conti@ieee.org

Abstract—Localization and navigation of passive objects enables new important applications in wireless environments. Monostatic sensor radar networks generate interesting solutions for passive localization and navigation in a variety of scenarios. In particular, ultrawide band (UWB) sensing provides fine delay resolution enabling high localization accuracy even in harsh propagation environments such as indoor. We develop a framework for design and analysis of passive navigation based on UWB monostatic sensor radar networks that relies on propagation environment and time-of-arrival estimation characterized by network experiments. As a case study, an UWB monostatic sensor radar network deployed in an indoor environment is considered, and the position of moving objects is inferred. In particular, Bayesian navigation based on particle filters implementation is employed and the role of mobility model for inferring target position is shown.

Index Terms—Passive tracking, TOA estimation, UWB, particle filters, mobility models.

I. INTRODUCTION

Network localization and navigation is an emerging paradigm that enables a variety of new important applications [1]. The localization and navigation process is referred to as active or passive depending on whether the objects to be localized infer their positions actively exchanging or passively backscattering signals, respectively [2].[1]

The operation of location-aware networks in harsh wireless propagation environments (e.g., indoor) is challenged by multipath, line-of-sight (LOS) blockage, excess delay propagation through materials, and clutter. In this conditions, ultrawide band (UWB) technology [4]–[6] can still provide accurate localization [7]–[9] due to its ability to solve multipath, penetrate obstacles, and provide accurate time-of-arrival (TOA) measurements [10]–[12].

Monostatic sensor radar networks extend the classical concept of single monostatic radar [13]–[17]. A clear understanding of how network configuration and propagation environment affect localization and navigation performance can be obtained through their characterization via network experimentation [18]. Several algorithms can be used to perform localization and navigation from TOA measurements available at each sensor radar. Here, we consider a Bayesian algorithm

based on particle filters (PFs) and mobility models to infer the position of a moving passive object [19]–[21].

In this paper, we present a framework for design and analysis of UWB monostatic sensor radar networks accounting for network configuration, multipath, obstructed line-of-sight (OLOS) propagation conditions, TOA estimation at each sensor algorithm, and particle filtering with mobility models for navigation. TOA estimation at each sensor is modeled based on network experiments. Built upon this, a Bayesian navigation algorithm with PF implementation is considered, which combines a prior knowledge based on mobility model with perception model and UWB ranging measurements. A case study in indoor environment is considered, where a UWB monostatic sensor radar network is deployed to infer the position of a passive object moving on various trajectories.

The remainder of the paper is organized as follows. Section II describes the sensor radar network model and Section III presents the TOA estimation algorithm. Section IV discusses the navigation algorithm and Section V quantifies the performance for the case study considered. Finally, our conclusion is given in Section VI.

II. NETWORK OF SENSOR RADARS

We now present the model and the assumptions for the UWB sensor radar network and its operation.

A. Sensing Network Topology

The radar configuration is defined by a set of N_S monostatic radars emitting and subsequently receiving a signal after backscattering on target object. Thus, signal TOA estimation is performed and the transmitter-to-target-to-receiver distance (signal path length) is determined.

For a target in position $\mathbf{p}$ and a monostatic radar $i = 1, ..., N_S$, the signal path length estimation is given by $\hat{d}_i(\mathbf{p}) = \hat{\tau}_i(\mathbf{p})\,c/2$, where c is the speed of light and $\hat{\tau}_i(\mathbf{p})$ is the estimated two-way TOA at the ith sensor relative to the signal backscattered by the target. It is well known that for monostatic radars, a temporal interval between signal transmission and reception is needed to resolve the system setup time, which is called blind range [22]. In the following, we will indicate with $\tau_{\min}$ the blind range which results in the minimum distance value $d^\star = \tau_{\min}\,c/2$. Therefore, a target can be detected and localized when $\hat{d}_i(\mathbf{p}) \geq d^\star$.

[1]Hybrid active and passive solutions can also be considered (see, e.g., [3]).

B. Backscattering Channel Modeling

The sensor radar detection and localization capabilities depend on the received waveform and signal-to-noise ratio (SNR). Specifically, the received SNR $\gamma_i(\mathbf{p})$ for radar i and target in $\mathbf{p}$ is given by

$$\gamma_i(\mathbf{p}) = \frac{P_{\mathrm{R},i}(\mathbf{p})}{\mathrm{PRF} N_0} \qquad (1)$$

where the received power $P_{\mathrm{R},i}(\mathbf{p})$ refers to a pulse repetition frequency (PRF) PRF and N_0 is the one-sided power spectral density (PSD) of thermal noise. Energy gathering of multiple target echoes enhances detection and TOA estimation. Specifically, N_{pulse} pulses are collected at the receiver.
The fulfillment of target detection and localization calls for a minimum received SNR $\gamma^\star$, which corresponds to a minimum received power $P_{\mathrm{R}}^\star$ as

$$P_{\mathrm{R},i}(\mathbf{p}) \geq P_{\mathrm{R}}^\star . \qquad (2)$$

In particular, the power received in a band $[f_{\mathrm{L}}, f_{\mathrm{U}}]$ by the ith sensor radar from the radar-to-target-to-radar path results in

$$P_{\mathrm{R},i}(\mathbf{p}) = \int_{f_{\mathrm{L}}}^{f_{\mathrm{U}}} R_i(f, \mathbf{p}) df \qquad (3)$$

where $R_i(f, \mathbf{p})$ is the one-sided received PSD at the ith sensor.

C. UWB Sensor Radar

The IEEE $802.15.4a$ channel model [11] is considered for both radar-to-target and target-to-radar paths. According to this, the one-sided PSD of the signal received by the ith radar is given by

$$\breve{R}_i(f, \mathbf{p}) = \frac{T_i(f) \eta_\mathrm{i}(f, \mathbf{\Theta}_\mathrm{i})^2 \Sigma(f)}{(4\pi)^3 \left(\frac{f_0 d_0}{c}\right)^2 \ell_i^{2\beta}(\mathbf{p}) \left(\frac{f}{f_0}\right)^{2\kappa+2}} \qquad (4)$$

where $T_i(f)$ is the transmitted PSD feeding the transmitting antenna; d_0 is a reference distance and f_0 the center frequency; $\eta_\mathrm{i}(f, \mathbf{\Theta}_\mathrm{i})$ is the antenna gain for the solid angle subtended between radar and target $\mathbf{\Theta}_\mathrm{i}$; $\Sigma(f)$ is the frequency-dependent radar cross section (RCS) of the target; and $\ell_i(\mathbf{p}) = d_i(\mathbf{p})/d_0$. The exponents β and κ provide the distance and frequency dependence of the path loss, respectively. Multipath propagation is modeled according to [23].

D. Walls Effects

In indoor environments, the received PSD can be also affected by an obstruction loss $L_i(f, \mathbf{p})$, which depends on the number and the type of obstructions (e.g., walls) present in the radar-to-target-to-radar path, as

$$R_i(f, \mathbf{p}) = \frac{\breve{R}_i(f, \mathbf{p})}{L_i(f, \mathbf{p})} . \qquad (5)$$

The obstruction loss (in dB) of a wall is defined in [18] as the path loss difference between two locations on the opposite sides of a wall, giving

$$L_i(f, \mathbf{p}) = \sum_{w=1}^{W_i(\mathbf{p})} 2\, n_{w,i}(\mathbf{p}) X_w(f) \qquad (6)$$

where $W_i(\mathbf{p})$ is the number of wall types crossed by the signal, $n_{w,i}(\mathbf{p})$ is the number of walls[2] of type w, and $X_w(f)$ is the frequency dependent loss for walls of type w. The minimum received power provides a maximum value $\ell_i^\star$ of $\ell_i(\mathbf{p})$, which limits the sensor coverage, by inverting (3).

The presence of obstacles and walls obstructing signal path has a two-fold effect: it results in an excess delay, which causes a positive bias on the TOA estimation and in an obstruction loss as in (6), which reduces the received SNR and increases the TOA estimation error. The quantification of these effects requires the characterization of the materials. Experimental results in [18] confirm that in the presence of concrete walls the TOA estimation bias (mean of the TOA estimation error) is $\mu_i(\mathbf{p}) \simeq \Delta/c$, where Δ is the total thickness of the wall.

III. TOA ESTIMATION

A variety of TOA estimators is present in the literature. In particular, those based on energy detection arised interest for their low complexity (sub-Nyquist sampling and non-coherent signal reception). In this case, the energy of received signal is determined in time intervals of duration T_{int} (energy bins) and then processed to estimate the TOA. A largely used solution consists in comparing energy bins with a threshold (i.e., threshold-based TOA estimator [12]).

The estimation $\hat{\tau}_i(\mathbf{p})$ of $\tau_i(\mathbf{p})$ for the sensor i is based on received waveform $r_i(t)$ and TOA estimator. Out-of-band noise and static clutter are mitigated by means of band-pass zonal and frame-to-frame filtering techniques. The output of the band-pass zonal filter (BPZF) and clutter removal provides to the energy detector (ED) an input signal (from transmission of N_{pulse} pulses) as given by

$$v_i(t) = \sum_{p=0}^{N_{\mathrm{pulse}}-1} \sum_{l=1}^{L} \alpha_i^{(l)}\, s(t - p\, T_{\mathrm{g}} - \tau_i^{(l)}) + n_i(t) \qquad (7)$$

where $s(t)$ is the pulse after BPZF, L is the number of received multipath components each with gain $\alpha_i^{(l)}$ and delay $\tau_i^{(l)}$, $T_{\mathrm{g}} = 1/\mathrm{PRF}$, and $n_i(t)$ is the filtered noise with one-sided PSD N_0.

The estimator uses a portion of the signal $v_i(t)$ consisting of N_{pulse} intervals each with duration T_{g} chosen to guarantee that each interval includes only one received pulse (thus avoiding ambiguous TOA estimations). Specifically, $\tau_i^{(1)} = \tau_i(\mathbf{p})$ and the goal is to estimate $\hat{\tau}_i^{(1)} = \hat{\tau}_i(\mathbf{p})$.[3] In the absence of prior information on target position, we consider $\tau_i^{(1)}$ uniformly distributed in $[0, T_{\mathrm{a}}]$, where T_{a} depends on the covered space and the PRF is chosen so that $T_{\mathrm{g}} > T_{\mathrm{a}}$. The observed signal $v_i(t)$ is the input of a square-law block followed by an integrate and dump (I&D) block with integration time T_{int}. Then, $N_{\mathrm{bin}} = \lfloor T_{\mathrm{g}}/T_{\mathrm{int}} \rfloor$ energy bins are collected (one each T_{int} seconds) in a decision vector. Each element of the vector is then compared with a threshold ξ_i. The choice of the threshold

---

[2]Note that in (6) the factor 2 accounts for the double pass of electromagnetic waves through the obstruction.

[3]Note that after perfect clutter removal, multipath propagation in (7) accounts for the paths backscattered by the target, which arrive at the receiver after reflections.

N_{pulse}	$\gamma_{\text{L}}^{\text{dB}}$	$\gamma_{\text{H}}^{\text{dB}}$	A	B
32	-4	12	21.93	-1.73
128	-1	15	27.13	-1.73
512	2	18	32.33	-1.73

ξ_i strongly affects the TOA estimation accuracy, detection probability, and false alarm probability.[4]

The estimated TOA $\hat{\tau}_i(\mathbf{p})$, is affected by an error that can be modeled as a Gaussian distributed random variable (RV), i.e. $\varepsilon_i(\mathbf{p}) \sim \mathcal{N}(\mu_i(\mathbf{p}), \sigma_i^2(\mathbf{p}))$ where the mean $\mu_i(\mathbf{p})$ accounts the presence of positive bias in obstructed path (it can be considered zero in LOS conditions) [12]. Specifically, the estimated TOA results in

$$\hat{\tau}_i(\mathbf{p}) = \tau_i \mathbf{p} + \varepsilon_i(\mathbf{p}) = \frac{2\, d_i(\mathbf{p})}{c} + \varepsilon_i(\mathbf{p})\,. \tag{8}$$

The standard deviation $\sigma_i(\mathbf{p})$ depends on the propagation environment, the TOA estimator, and the received SNR $\gamma_i(\mathbf{p})$. In general, $\sigma_i(\mathbf{p})$ is a non-increasing function of the received SNR.[5] For TOA estimation based on energy detection, three different working regions are experienced. In particular, the regions of small and large SNR values correspond to asymptotic regions of large and small standard deviation $\sigma_i(\gamma_i)$, respectively, while a transition zone is present for moderate SNR values. Such behavior can be approximated by

$$\log_{10}(\sigma_i) \simeq \begin{cases} \log_{10}\left(\frac{T_{\text{a}}}{\sqrt{12}}\right) & \gamma_i^{\text{dB}} < \gamma_{\text{L}}^{\text{dB}} \\ z_\sigma(\gamma_i) & \gamma_{\text{L}}^{\text{dB}} \leq \gamma_i^{\text{dB}} \leq \gamma_{\text{H}}^{\text{dB}} \\ \log_{10}\left(\frac{T_{\text{int}}}{\sqrt{12}}\right) & \gamma_i^{\text{dB}} > \gamma_{\text{H}}^{\text{dB}} \end{cases} \tag{9}$$

where the SNR thresholds $\gamma_{\text{L}}^{\text{dB}}$ and $\gamma_{\text{H}}^{\text{dB}}$ shape the small and large SNR regions, respectively.[6] A good approximation for $z_\sigma(\gamma_i)$ is given by $z_\sigma(\gamma_i) \approx \text{A} + \text{B} \cdot 10\log_{10}(\gamma_i)$ where the parameters A and B can be easily determined according to $T_{\text{int}}, T_{\text{a}}, \gamma_{\text{L}}^{\text{dB}}$, and $\gamma_{\text{H}}^{\text{dB}}$. Examples are reported in Table III for $T_{\text{int}} = 4\text{ns}$ and $T_{\text{a}} = 100\text{ns}$.

IV. Navigation Algorithm

The aim of a navigation algorithm is to estimate the target position $\mathbf{p}^{(k)}$ at each time index k (i.e., the states) from a set of observations $\hat{\mathbf{d}}^{(k)}$ (i.e., $\hat{\mathbf{d}}^{(k)}$ is the vector of estimated distances $\hat{d}_i(\mathbf{p}^{(k)}) = \hat{\tau}_i(\mathbf{p}^{(k)})\,c/2$). The Bayesian inference of position's belief $b(\mathbf{p}^{(k)}) = p(\mathbf{p}^{(k)}|\hat{\mathbf{d}}^{(1:k)})$ (i.e., posterior distribution of the position state vector, given past and current observations from time index 1 to k) is obtained in two phases: (i) a *prediction* phase in which the belief is determined based on previous position and a mobility model, and (ii) an *update* phase where the belief is updated based on new measurements and a perception model. Therefore, by denoting with $\hat{\mathbf{d}}^{(1:k)}$ the

---

set of available observations at time index k, $b(\mathbf{p}^{(k)})$ is given by

$$b(\mathbf{p}^{(k)}) = \frac{b^-(\mathbf{p}^{(k)})\, p(\hat{\mathbf{d}}^{(k)}|\mathbf{p}^{(k)})}{p(\hat{\mathbf{d}}^{(k)}|\hat{\mathbf{d}}^{(1:k-1)})} \tag{10}$$

where the predicted belief $b^-(\mathbf{p}^{(k)}) = p(\mathbf{p}^{(k)}|\hat{\mathbf{d}}^{(1:k-1)})$ is

$$b^-(\mathbf{p}^{(k)}) = \int p(\mathbf{p}^{(k)}|\mathbf{p}^{(k-1)})b(\mathbf{p}^{(k-1)})\, d\mathbf{p}^{(k-1)}\,. \tag{11}$$

The term $p(\mathbf{p}^{(k)}|\mathbf{p}^{(k-1)})$ is the mobility model of the target and gives the probability distribution function (PDF) of being in $\mathbf{p}^{(k)}$ conditioned on previous position $\mathbf{p}^{(k-1)}$. The belief (11) is predicted according to previous state and mobility model, then updated according to (10) and new measurements. Finally the estimated position $\hat{\mathbf{p}}^{(k)}$ is determined as that value that maximizes $b(\mathbf{p}^{(k)})$ in (10). Various implementations of Bayesian inference are possible, which differ in the beliefs computation. In particular, we consider the PF algorithm [20], [21].

A. Particle Filtering

The key idea of PFs is to represent the posterior belief (distribution), by a set of random samples (particles) as

$$b(\mathbf{p}^{(k)}) \approx \sum_{p=1}^{N_{\text{p}}} w_{k,p}\delta(\mathbf{p}^{(k)} - \mathbf{p}_p^{(k)}) \tag{12}$$

where N_{p} is the number of particles, $\delta(\cdot)$ is the Delta function, and $w_{k,p} \geq 0 \ \forall k,p$ is the weight for particle s at time index k, with $\sum_{p=1}^{N_{\text{p}}} w_{k,p} = 1$. The weights are chosen using the principle of importance sampling in which the more dense are the samples, the more probable the object is located [19], [21]. Specifically, the main important recursive steps for evaluating the sth particle can be summarized as follow

$$\mathbf{p}_p^{(k)} \sim p(\mathbf{p}^{(k)}|\mathbf{p}_p^{(k-1)}) \tag{13}$$

$$w_{k,p} = w_{k-1,p}\, p(\hat{\mathbf{d}}^{(k)}|\mathbf{p}_p^{(k)})\,. \tag{14}$$

B. Mobility and Perception Models

A Gaussian mobility model is considered as given by

$$p(\mathbf{p}^{(k)}|\mathbf{p}^{(k-1)}) = \frac{1}{\sqrt{2\pi}\sigma_{\text{m}}} e^{-\frac{\left\|\mathbf{p}^{(k)} - \boldsymbol{\mu}_k\right\|^2}{2\sigma_{\text{m}}^2}} \tag{15}$$

where the standard deviation σ_{m} considers the uncertainty on the target movement, and the mean $\boldsymbol{\mu}_k$ depends on $\mathbf{p}^{(k-1)}$. We consider two different mobility model: the speed known direction unknown (SKDU) and the speed and direction learning (SDL).

In the SKDU model, the target speed intensity is known but there are no direction information. Therefore,

$$\boldsymbol{\mu}_k = \hat{\mathbf{p}}^{(k-1)} + \mathbf{v}_k\, T \tag{16}$$

where the orientation angle of the speed vector $\mathbf{v}$ is uniformly distributed in $[-\pi,\pi]$ and T is the time between two consecutive measurements.

---

[4]The design of the threshold is outside the focus of the paper.

[5]In the following we will remove the dependence of σ_i and γ_i on $\mathbf{p}$ to simplify the notation.

[6]Notation x^{dB} stands for $10\log_{10}(x)$.

In the SDL model the speed vector is determined from previously estimated positions as

$$\mathbf{v}_{k-1} = \frac{1}{N_v T} \sum_{v=1}^{N_v} \left(\hat{\mathbf{p}}^{(k-v)} - \hat{\mathbf{p}}^{(k-v-1)} \right) \qquad (17)$$

where N_v is the length of a sliding window of previous states. Therefore,

$$\boldsymbol{\mu}_k = \hat{\mathbf{p}}^{(k-1)} + \mathbf{v}_{k-1} \, T \qquad (18)$$

For what concerns the perception model, we consider independent observations. Thus,

$$p(\hat{\mathbf{d}}^{(k)}|\mathbf{p}^{(k)}) = \prod_{i=1}^{N_S} p(\hat{d}_i^{(k)}|\mathbf{p}^{(k)}) \qquad (19)$$

where $\hat{d}_i^{(k)}$ is the measurement from the ith radar at time index k. We consider a perception model with Gaussian distribution as given by

$$p(\hat{d}_i^{(k)}|\mathbf{p}^{(k)}) = \frac{1}{\sqrt{2\pi}\sigma_{\mathrm{p}}} e^{-\frac{\left(\hat{d}_i^{(k)} - \left\|\mathbf{p}^{(k)} - \mathbf{s}_i\right\|\right)^2}{2\sigma_{\mathrm{p}}^2}}. \qquad (20)$$

where $\mathbf{s}_i$ is the position of the ith sensor and the standard deviation σ_{p} depends on both the localization technique and propagation conditions.

V. CASE STUDY

We consider a network of monostatic sensor radars composed by 10 nodes deployed in an indoor environment as shown in Fig. 1. A target moves along 5 different random trajectories, each of length 20m, with speed intensity $v = 1$m/s. To compare the performance in the case study environment with that in LOS conditions, the same environment area and nodes deployment as Fig. 1 have been considered also in the absence of walls. Navigation performance is given in terms of navigation error outage (NEO), which is the probability that the navigation error falls above a given target value e_{th} as

$$\begin{aligned} P_{\mathrm{NEO}} &= \mathbb{P}\{e(\mathbf{p}^{(k)}) > e_{\mathrm{th}}\} \qquad (21) \\ &= \mathbb{E}\left\{ \mathbb{1}_{(e_{\mathrm{th}}, +\infty)} \left(e(\mathbf{p}^{(k)}) \right) \right\} \end{aligned}$$

where $\mathbb{1}_{\mathcal{B}}(x) \triangleq 1$ if $x \in \mathcal{B}$ and 0 otherwise, and the navigation error, for each time index k, is given by

$$e(\mathbf{p}^{(k)}) = \|\hat{\mathbf{p}}^{(k)} - \mathbf{p}^{(k)}\| \qquad (22)$$

which is the Euclidean distance between the target estimated position $\hat{\mathbf{p}}^{(k)}$ and the true position $\mathbf{p}^{(k)}$.

Results are given for both SKDU and SDL mobility models, with $N_v = 5$, $\sigma_{\mathrm{p}} = 1$m and $\sigma_{\mathrm{m}} = 0.8$m. Specifically, the value of σ_{m} is such that with probability 0.9 the new position is within a circle centered in $\boldsymbol{\mu}_k$ of radius vT.

We consider impulse radio UWB sensor radars transmitting a sequence of pulses with $\mathsf{PRF} = 5$ MHz. The transmitted PSD is $T_i(f) = -42$ dBm/MHz over the frequency band $[f_{\mathrm{L}}, f_{\mathrm{L}} + B]$ and 0 otherwise, where $f_{\mathrm{L}} = 3.1$ GHz
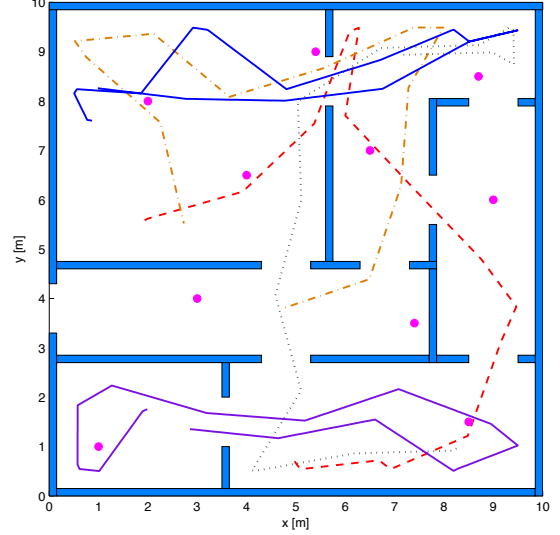

Fig. 1. Environment, 10 sensor radars (magenta), and 5 trajectories considered as case study.

and $B = 1.7$ GHz,[7] the noise power spectral density is $N_0 = -200$ dBW/Hz, and antennas are omnidirectional. In (4), $d_0 = 1$ m, $f_0 = f_{\mathrm{L}} + B/2$, and $\kappa = 0$. The path-loss exponent is $\beta = 2$ and obstruction path effects are accounted for through (6). The minimum received power (received sensitivity) is $P_{\mathrm{R}}^{\star} = -100$ dBm.

The channel impulse response is composed by $L_{\mathrm{p}} = 20$ paths spaced by $\delta_{\mathrm{p}} = 4$ns with exponential power delay profile $\epsilon = 20$ ns, Rayleigh distributed path amplitudes, and delay spread 16.6 ns [23]. A Swerling type-III RCS is considered [22], which models a human target as a Chi-squared distributed RV Σ with four degrees of freedom, constant during a scan (i.e., the transmission of N_{pulse} pulses necessary for the whole TOA estimation process) and independent from scan to scan. The mean RCS is $\mathbb{E}\{\Sigma\} = 1$ m^2, which is typical for the human body [24].

The ED based TOA estimation $\hat{\tau}_i(\mathbf{p})$ for each sensor radar adopt an integration time $T_{\mathrm{int}} = 4$ ns and we consider $T_{\mathrm{a}} = 100$ ns. Unless otherwise stated, the number of accumulated received pulses is $N_{\mathrm{pulse}} = 128$. Static clutter removal technique based on a simple frame-to-frame algorithm is performed from the received waveform [25]. In the TOA estimator, each threshold ξ_i is found through exhaustive *a posteriori* search, as the value that minimizes the average RMSE of TOA estimation, averaged over the channel statistic, for each SNR.[8]

---

[7]This is compliant to the European lower band.

[8]Alternatively, in [26] a simple criterium to determine a threshold is proposed based on the evaluation of the probability of early detection and noise power knowledge. A blind TOA estimation which gives near-optimal performance without the need to setup a threshold is proposed in [27].
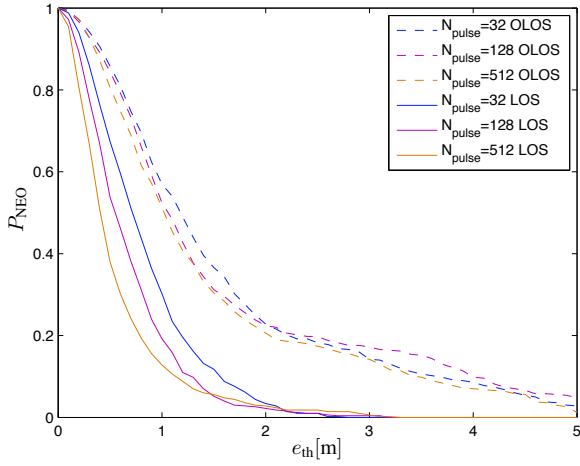
Fig. 2. NEO over all 5 random trajectories for different values of N_{pulse} with $T_{int} = 4$ns.

Fig. 4. NEO over all 5 trajectories for SKDU and SDL mobility models and different values of T, $T_{int} = 4$ns, and $N_{pulse} = 128$.
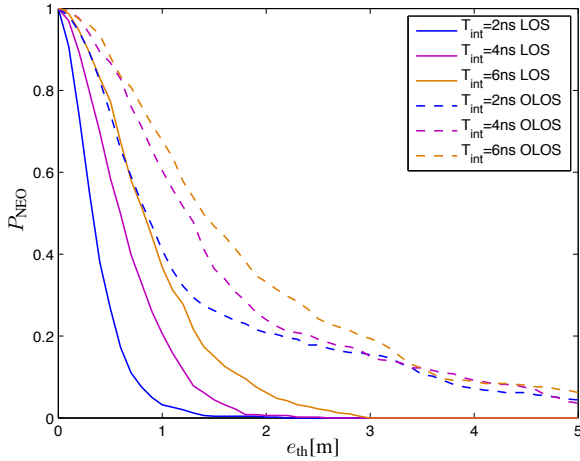

Fig. 3. NEO over all 5 random trajectories for different values of T_{int} with $N_{pulse} = 128$.

A. Effects of TOA Estimation

The effects of ED setting on navigation accuracy are shown in Fig. 2 and Fig. 3, where the NEO dependence on N_{pulse} and T_{int} is shown, respectively. The NEO is obtained over all 5 random trajectories by considering $T = 0.2$s and SKDU mobility model in LOS and OLOS conditions. Specifically, for LOS conditions in the 80% of cases the navigation error is below 0.8m, 1m, 1.2m for $N_{pulse} = 32, 128, 512$, respectively (Fig. 2) and below 0.6m, 0.9m, 1.5m for $T_{int} = 2, 4, 6$ ns, respectively (Fig. 3). For OLOS conditions in the 80% of cases the navigation error is below 2m, 2.3m, 2.3m for $N_{pulse} = 32, 128, 512$, respectively (Fig. 2), and below 2.3m, 2.5m, 2.9m for $T_{int} = 2, 4, 6$ ns, respectively (Fig. 3).

B. Effects of Perception and Mobility Models

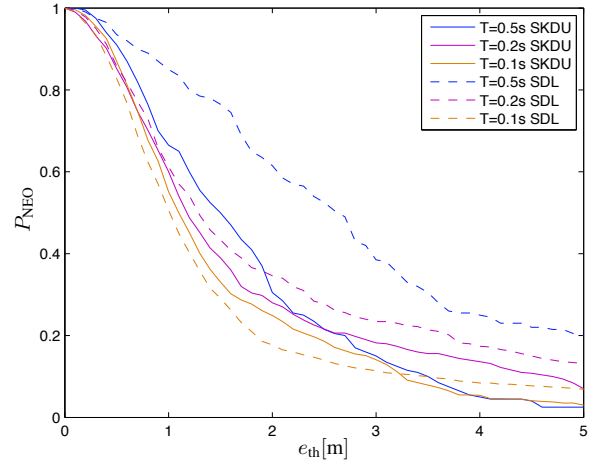Figure 4 shows the NEO for the two mobility models and different time intervals between two different observations in OLOS conditions. Here, $T_{int} = 4$ns and $N_{pulse} = 128$ are considered. For $T = 0.5$s the SKDU mobility model provides the best solution since in the 80% of the cases the error is below 2.7m for the SKDU and 5m for the SDL. For $T = 0.2$s in the 80% of the cases the error is below 2.7m for both the mobility models, even if the speed of the target is unknown in the SDL. For $T = 0.1$s, the SDL shows best performance with respect to the SKDU. Specifically, the SKDU mobility model shows better performance for low TOA estimation update rate $1/T$ since the speed intensity is known, while the speed estimated by SDL is inaccurate. Differently, the more often the position is estimated the more accurate is the speed estimate and direction estimate of the SDL model, which indeed shows better performance than SKDU (in which no information and learning algorithms about direction are exploited).

VI. CONCLUSION

A framework for design and analysis of UWB monostatic radar sensor networks for passive localization and navigation is presented. The framework accounts for the network setting, environment propagation, TOA estimation techniques, and Bayesian navigation algorithms. Navigation techniques based on particle filter algorithm and mobility models have been compared in terms of navigation error outage for a case study in an indoor environment with both LOS and OLOS conditions. It is shown that mobility model and TOA estimation algorithms significantly affect the performance in harsh environments.

REFERENCES

[1] M. Z. Win, A. Conti, S. Mazuelas, Y. Shen, W. M. Gifford, D. Dardari, and M. Chiani, "Network localization and navigation via cooperation," *IEEE Commun. Mag.*, vol. 49, no. 5, pp. 56–62, May 2011.
[2] D. Dardari, R. D'Errico, C. Roblin, A. Sibille, and M. Z. Win, "Ultrawide bandwidth RFID: The next generation?" *Proc. IEEE*, vol. 99, no. 7, pp. 1570–1582, Jul. 2010, special issue on *RFID - A Unique Radio Innovation for the 21st Century*.

[3] L. Reggiani and R. Morichetti, "Hybrid active and passive localization for small targets," in *Indoor Positioning and Indoor Navigation (IPIN), 2010 International Conference on*, Sep. 2010, pp. 1 –5.

[4] M. Z. Win and R. A. Scholtz, "Impulse radio: How it works," *IEEE Commun. Lett.*, vol. 2, no. 2, pp. 36–38, Feb. 1998.

[5] ——, "Ultra-wide bandwidth time-hopping spread-spectrum impulse radio for wireless multiple-access communications," *IEEE Trans. Commun.*, vol. 48, no. 4, pp. 679–691, Apr. 2000.

[6] L. Yang and G. B. Giannakis, "Ultra-wideband communications: An idea whose time has come," *IEEE Signal Process. Mag.*, vol. 21, no. 6, pp. 26–54, Nov. 2004.

[7] Y. Shen, H. Wymeersch, and M. Z. Win, "Fundamental limits of wideband localization – Part II: Cooperative networks," *IEEE Trans. Inf. Theory*, vol. 56, no. 10, pp. 4981–5000, Oct. 2010. [Online]. Available: http://arxiv.org/abs/1006.0890v1

[8] S. Gezici, Z. Tian, G. B. Giannakis, H. Kobayashi, A. F. Molisch, H. V. Poor, and Z. Sahinoglu, "Localization via ultra-wideband radios: a look at positioning aspects for future sensor networks," *IEEE Signal Process. Mag.*, vol. 22, no. 4, pp. 70–84, Jul. 2005.

[9] Y. Shen and M. Z. Win, "Fundamental limits of wideband localization – Part I: A general framework," *IEEE Trans. Inf. Theory*, vol. 56, no. 10, pp. 4956–4980, Oct. 2010. [Online]. Available: http://arxiv.org/abs/1006.0888v1

[10] M. Z. Win and R. A. Scholtz, "Characterization of ultra-wide bandwidth wireless indoor communications channel: A communication theoretic view," *IEEE J. Sel. Areas Commun.*, vol. 20, no. 9, pp. 1613–1627, Dec. 2002.

[11] A. F. Molisch, D. Cassioli, C.-C. Chong, S. Emami, A. Fort, B. Kannan, J. Karedal, J. Kunisch, H. Schantz, K. Siwiak, and M. Z. Win, "A comprehensive standardized model for ultrawideband propagation channels," *IEEE Trans. Antennas Propag.*, vol. 54, no. 11, pp. 3151–3166, Nov. 2006, special issue on *Wireless Communications*.

[12] D. Dardari, A. Conti, U. J. Ferner, A. Giorgetti, and M. Z. Win, "Ranging with ultrawide bandwidth signals in multipath environments," *Proc. IEEE*, vol. 97, no. 2, pp. 404–426, Feb. 2009, special issue on *Ultra-Wide Bandwidth (UWB) Technology & Emerging Applications*.

[13] A. Haimovich, R. Blum, and L. Cimini, "MIMO radar with widely separated antennas," *Signal Processing Magazine, IEEE*, vol. 25, no. 1, pp. 116 –129, Jan. 2008.

[14] Y. Zhou, C. L. Law, Y. L. Guan, and F. Chin, "Localization of passive target based on UWB backscattering range measurement," in *Proc. IEEE Int. Conf. on Ultra-Wideband (ICUWB 2009)*, Vancouver, CANADA, Sep. 2009, pp. 145–149.

[15] E. Paolini, A. Giorgetti, M. Chiani, R. Minutolo, and M. Montanari, "Localization capability of cooperative anti-intruder radar systems," *EURASIP J. Adv. in Signal Process.*, vol. 2008, pp. 1–14, 2008.

[16] S. Bartoletti, A. Conti, and A. Giorgetti, "Analysis of UWB radar sensor networks," in *Proc. IEEE Int. Conf. on Commun.*, Cape Town, South Africa, May 2010.

[17] S. Bartoletti and A. Conti, "Passive network localization via UWB wireless sensor radars: the impact of TOA estimation," in *Proc. IEEE Int. Conf. on Ultra-Wideband (ICUWB)*, Bologna, Italy, Sep. 2011, pp. 576–580.

[18] A. Conti, M. Guerra, D. Dardari, N. Decarli, and M. Z. Win, "Network experimentation for cooperative localization," *IEEE J. Sel. Areas Commun.*, vol. 30, no. 2, pp. 467–475, Feb. 2012.

[19] R. Douc and O. Cappe, "Comparison of resampling schemes for particle filtering," in *Image and Signal Processing and Analysis, 2005. ISPA 2005. Proceedings of the 4th International Symposium on*, Sep. 2005, pp. 64 – 69.

[20] F. Gustafsson, F. Gunnarsson, N. Bergman, U. Forsell, J. Jansson, R. Karlsson, and P. J. Nordlund, "Particle filters for positioning, navigation and tracking," *IEEE Trans. Signal Process.*, vol. 50, no. 2, pp. 425–437, Feb. 2002.

[21] M. S. Arulampalam, S. Maskell, N. Gordon, and T. Clapp, "A tutorial on particle filters for online nonlinear/non-Gaussian Bayesian tracking," *IEEE Trans. Signal Process.*, vol. 50, no. 2, pp. 174–188, Feb. 2002.

[22] M. I. Skolnik, *Radar Handbook*, 2nd ed. McGraw-Hill Professional, Jan. 1990.

[23] D. Cassioli, M. Z. Win, and A. F. Molisch, "The ultra-wide bandwidth indoor channel: From statistical model to simulations," *IEEE J. Sel. Areas Commun.*, vol. 20, no. 6, pp. 1247–1257, Aug. 2002.

[24] B. Boudamouz, P. Millot, and C. Pichot, "Through the wall MIMO radar detection with stepped frequency waveforms," in *Proc. European Radar Conference (EuRAD)*, Paris, France, Sep. 2010, pp. 400–402.

[25] S. Nag and M. Barnes, "A moving target detection filter for an ultra-wideband radar," in *Proc. IEEE Int. Radar Conf. (RadarCon)*, Huntsville, Ala, USA, May 2003, pp. 147–153.

[26] D. Dardari, C.-C. Chong, and M. Z. Win, "Threshold-based time-of-arrival estimators in UWB dense multipath channels," *IEEE Trans. Commun.*, vol. 56, no. 8, pp. 1366–1378, Aug. 2008.

[27] A. Giorgetti and M. Chiani, "A new approach to time-of-arrival estimation based on information theoretic criteria," in *Proc. IEEE Int. Conf. on Ultra-Wideband (ICUWB)*, Bologna, ITALY, Sep. 2011, pp. 460–464.